

# The effects of Mn concentration on spin-polarized transport through ZnSe/ZnMnSe/ZnSe heterostructures

Alireza Saffarzadeh\*

*Department of Physics, Tehran Payame Noor University,  
Fallahpour St., Nejatollahi St., Tehran, Iran*

(Dated: September 3, 2018)

## Abstract

We have studied the effects of Mn concentration on the ballistic spin-polarized transport through diluted magnetic semiconductor heterostructures with a single paramagnetic layer. Using a fitted function for zero-field conduction band offset based on the experimental data, we found that the spin current densities strongly depend on the Mn concentration. The magnitude as well as the sign of the electron-spin polarization and the tunnel magnetoresistance can be tuned by varying the Mn concentration, the width of the paramagnetic layer, and the external magnetic field. By an appropriate choice of the Mn concentration and the width of the paramagnetic layer, the degree of spin polarization for the output current can reach 100% and the device can be used as a spin filter.

---

\*Corresponding author. E-mail: a-saffar@tehran.pnu.ac.ir

## I. INTRODUCTION

Recent advances in controlling the spin-polarized transport in metallic magnetic structures, and successful applications of such systems in electronic devices [1, 2] renewed world-wide interest in diluted magnetic semiconductor (DMS) structures. These materials are a promising component for the new spin-based information technology, in which the spin degree of freedom of the electron can be utilized to sense, store, process and transfer information. II-VI DMSs [3, 4], are a class of materials that has received much attention in recent years due to their interesting physical properties and the potential applications in integrated magneto-optoelectronic devices [5]. They are known to be good candidates for effective spin injection into a nonmagnetic semiconductor (NMS) because their spin polarization is nearly 100% and their conductivity is comparable to that of typical NMS. Among different types of II-VI DMSs, (Zn,Mn)Se is a very promising one for spin injection, which has been previously used for spin injection experiments into GaAs [6], and ZnSe [7, 8, 9].

All  $A_{1-x}^{II}Mn_xB^{VI}$  alloys are direct-gap semiconductors like their  $A^{II}B^{VI}$  parent materials. In the presence of a magnetic field, the band edges in these materials undergo a huge spin splitting due to the  $sp - d$  exchange between carriers and localized magnetic ions [4], while the splitting in the nonmagnetic layers is much smaller. When the large Zeeman splitting in the magnetic layers overcomes the band offsets in both conduction and valance bands, the magnetic layers act as barriers for electrons and holes in the spin-up state, and as quantum wells for the spin-down state.

In recent years, the spin-polarized transport in II-VI DMS heterostructures has been investigated theoretically. Based on a quantum theory and the free-electron approximation, Egues [10], Guo *et al.* [11], and Chang and Peeters [12] studied spin filtering in ZnSe/Zn<sub>1-x</sub>Mn<sub>x</sub>Se/ZnSe heterostructures in the ballistic region. The results showed a strong suppression for one of the spin components of the current density with increasing the external magnetic field. Also, Zhai *et al.* [13] investigated the effects of conduction band offset on the spin transport in such heterostructures and showed that the positive zero-field band offset can drastically increase the spin polarization. However, they have not considered the effects of Mn concentration and the width of the paramagnetic layer on the spin-polarized transport. Thus other aspects of these heterostructures remain to be explained.

In the present work, we study theoretically the dependence of spin-polarized transport

on Mn concentration in ZnSe/ZnMnSe/ZnSe structures. The ZnSe layers are considered as emitter and collector attached to external leads. We assume that the carrier wave vector parallel to the interfaces and the carrier spin are conserved in the tunneling process through the whole system. These assumptions can be well justified for interfaces between materials whose lattice constants are nearly equal; and when the sample dimensions are much smaller than the spin coherence length. Using a quantum theory, we study the effects of Mn concentration and the width of the paramagnetic layer on spin-dependent current densities, the degree of spin polarization, and the magnetoresistance ratio.

In section 2, we present a fitted function for zero-field conduction band offset and describe the model. Then, the spin current densities, the electron-spin polarization, and the magnetoresistance ratio for ZnSe/ZnMnSe/ZnSe heterostructures are formulated. In section 3, the numerical results for the above quantities are discussed in terms of the Mn concentration, the width of the paramagnetic layer, and the applied voltage. The results of this work are summarized in section 4.

## II. MODEL AND FORMALISM

Consider a spin unpolarized electron current injected into ZnSe/Zn<sub>1-x</sub>Mn<sub>x</sub>Se/ZnSe structures in the presence of magnetic and electric fields along the growth direction (taken as  $z$  axis). In Mn-based DMS systems, the conduction electrons that contribute to the electric currents, interact with the 3d<sup>5</sup> electrons of the Mn ions with spin  $S = \frac{5}{2}$  via the sp-d exchange interaction. Due to the sp-d exchange interaction, the external magnetic field gives rise to the spin splitting of the conduction band states in the Zn<sub>1-x</sub>Mn<sub>x</sub>Se layer. Therefore, the injected electrons see a spin-dependent potential. In the framework of the parabolic-band effective mass approximation, the one-electron Hamiltonian of such system can be written as

$$H = \frac{1}{2m^*}(\mathbf{P} + e\mathbf{A})^2 + V_s + V_x(z) + V_{\sigma_z}(z) - \frac{eV_a z}{d}, \quad (1)$$

where the electron effective mass  $m^*$  is assumed to be identical in all the layers, and the vector potential is taken as  $\mathbf{A} = (0, Bx, 0)$ . Here,  $V_s = \frac{1}{2}g_s\mu_B\sigma \cdot \mathbf{B}$  describes the Zeeman splitting of the conduction electrons, where  $\sigma$  is the conventional Pauli spin operator;  $V_x(z)$  is the heterostructure potential or the conduction band offset in the absence of a magnetic field, which depends on the Mn concentration  $x$  and is the difference between the conduction

band edge of the  $\text{Zn}_{1-x}\text{Mn}_x\text{Se}$  layer and that of the  $\text{ZnSe}$  layer;  $V_{\sigma_z}(z)$  is the sp-d exchange interaction between the spin of injected electron and the spin of Mn ions and can be calculated within the mean field approximation. Hence, the sum of the last two terms can be written as

$$V_x(z) + V_{\sigma_z}(z) = [(1/2)\Delta E(x) - N_0\alpha\sigma_z x_{eff}\langle S_z \rangle]\Theta(z)\Theta(d-z), \quad (2)$$

where

$$\Delta E(x) = -0.63x + 22x^2 - 195x^3 + 645x^4. \quad (3)$$

Here,  $\Delta E(x) (= E_g(x) - E_g(0))$  is the sum of the conduction and valance band offset under zero magnetic field, when the real Mn concentration is  $x$ . In Fig. 1, we have shown the Mn concentration dependence of the energy gap  $E_g(x)$  in  $\text{Zn}_{1-x}\text{Mn}_x\text{Se}$  layer. It is clear that the band gap of  $\text{Zn}_{1-x}\text{Mn}_x\text{Se}$  varies anomalously with  $x$ ; it shows a minimum at  $x \sim 0.02$  and increases linearly with  $x$  for  $x \geq 0.05$ . This anomalous behavior of  $\text{Zn}_{1-x}\text{Mn}_x\text{Se}$  which called band-gap bowing, probably refers to the sp-d exchange interaction [4]. In deriving  $\Delta E(x)$ , we have used of the fitted curve of  $E_g(x)$ . We have approximated  $\Delta E(x)/2$  as the zero-field conduction band offset. This function does not depend on spin, and for  $x \leq 0.043$  behaves as a quantum well, and as a potential barrier for  $x \geq 0.043$ .

In Eq. (2),  $N_0\alpha$  is the electronic sp-d exchange constant,  $\sigma_z = \pm 1/2$  (or  $\uparrow, \downarrow$ ) are the electron spin components along the magnetic field,  $x_{eff} = x(1-x)^{12}$  is the effective Mn concentration used to account for antiferromagnetic Mn-Mn coupling, and  $\Theta(z)$  is the step function.  $\langle S_z \rangle$  is the thermal average of  $z$ th component of  $\text{Mn}^{2+}$  spin in the paramagnetic layer which is given by the modified  $\frac{5}{2}$  Brillouin function  $SB_S[5\mu_B B/k_B(T + T_0)]$ , where  $T_0$  is an empirical parameter representing antiferromagnetic interactions between the Mn ions [15]. The last term in Eq. (1) denotes the effect of an applied voltage  $V_a$  along the  $z$  axis on the system, and  $d$  is the width of the paramagnetic layer. It is important to note that,  $d$  is much smaller than the spin coherence length in the semiconductors. Therefore, we have neglected the effects of spin-flip processes in the Hamiltonian of the system.

In the absence of any kind of scattering center for the electrons, the motion along the  $z$ -axis is decoupled from that of the  $x$ - $y$  plane. Therefore, in the presence of magnetic field  $B$ , the in-plane motion is quantized in Landau levels with energies  $E_n = (n + 1/2)\hbar\omega_c$ , where  $n = 0, 1, 2, \dots$  and  $\omega_c = eB/m^*$ . In such case, the motion of electrons along the  $z$  axis can

be reduced to the following one-dimensional (1D) Schrödinger equation

$$-\frac{\hbar^2}{2m^*} \frac{d^2 \psi_{\sigma_z}(z)}{dz^2} + U_{\sigma_z}(z, B) \psi_{\sigma_z}(z) = E_z \psi_{\sigma_z}(z), \quad (4)$$

where  $E_z$  is the longitudinal energy of electrons and  $U_{\sigma_z}(z, B) = V_s + V_x(z) + V_{\sigma_z}(z) - eV_a z/d$  is the effective potential seen by a traverse electron, which includes the effects of spin, conduction band offset, and external magnetic and electric fields. The general solution to the above Schrödinger equation is as follows:

$$\psi_{j\sigma_z}(z) = \begin{cases} A_{1\sigma_z} e^{ik_{1\sigma_z} z} + B_{1\sigma_z} e^{-ik_{1\sigma_z} z}, & z < 0, \\ A_{2\sigma_z} \text{Ai}[\rho_{\sigma_z}(z)] + B_{2\sigma_z} \text{Bi}[\rho_{\sigma_z}(z)], & 0 < z < d, \\ A_{3\sigma_z} e^{ik_{3\sigma_z} z} + B_{3\sigma_z} e^{-ik_{3\sigma_z} z}, & z > d, \end{cases} \quad (5)$$

where  $k_{1\sigma_z} = \sqrt{2m^*(E_z - V_s)}/\hbar$ ,  $k_{3\sigma_z} = \sqrt{2m^*(E_z - V_s + eV_a)}/\hbar$ ;  $\text{Ai}[\rho_{\sigma_z}(z)]$  and  $\text{Bi}[\rho_{\sigma_z}(z)]$  are Airy functions with  $\rho_{\sigma_z}(z) = [d/(eV_a\lambda)](E_z - U_{\sigma_z})$ , and  $\lambda = [-\hbar^2 d/(2m^* eV_a)]^{1/3}$ ;  $A_{j\sigma_z}$  and  $B_{j\sigma_z}$  (with  $j=1-3$ ) are constants which can be obtained by matching the wave functions and their derivatives at the interfaces of  $\text{Zn}_{1-x}\text{Mn}_x\text{Se}$  and  $\text{ZnSe}$  layers. The matching results in a system of equations, which can be represented in a matrix form [16],

$$\begin{pmatrix} A_{1\sigma_z} \\ B_{1\sigma_z} \end{pmatrix} = M_1^{-1}(0) M_2(0) M_2^{-1}(d) M_3(d) \begin{pmatrix} A_{3\sigma_z} \\ B_{3\sigma_z} \end{pmatrix} \\ = M_{total} \begin{pmatrix} A_{3\sigma_z} \\ B_{3\sigma_z} \end{pmatrix}. \quad (6)$$

Here,  $M_{total}$  is the transfer matrix that connects the incidence and transmission amplitudes, and

$$M_j(z_i) = \begin{pmatrix} \psi_j^+(z) & \psi_j^-(z) \\ \frac{d\psi_j^+(z)}{dz} & \frac{d\psi_j^-(z)}{dz} \end{pmatrix}_{z=z_i}, \quad (7)$$

where,  $\psi_j^+(z)$  and  $\psi_j^-(z)$  are, respectively, the first and second term of the wave functions in each layer, without considering their coefficients. Therefore, the transmission coefficient of the spin  $\sigma_z$  electron, which is defined as the ratio of the transmitted flux in the collector to the incident flux in the emitter, can be written as

$$T_{\sigma_z}(E_z, B, V_a) = \frac{k_{3\sigma_z}}{k_{1\sigma_z}} \left| \frac{1}{M_{total}^{11}} \right|^2, \quad (8)$$

where  $M_{total}^{11}$  is the (1,1) element of the matrix  $M_{total}$ . The spin-dependent current density can be determined by

$$J_{\sigma_z}(B) = J_0 B \sum_{n=0}^{\infty} \int_0^{+\infty} T_{\sigma_z}(E_z, B, V_a) \times \{f[E_z + (n + \frac{1}{2})\hbar\omega_c + V_s] - f[E_z + (n + \frac{1}{2})\hbar\omega_c + V_s + eV_a]\} dE_z, \quad (9)$$

where  $J_0 = e^2/4\pi^2\hbar^2$ ,  $f(E) = 1/\{1 + \exp[(E - E_F)/k_B T]\}$  is the Fermi-Dirac distribution function in which  $k_B$  is the Boltzmann constant,  $T$  is the temperature, and  $E_F$  denotes the emitter Fermi energy.

The degree of spin polarization for electrons traversing the heterostructure is defined by

$$P = \frac{J_{\downarrow}(B) - J_{\uparrow}(B)}{J_{\downarrow}(B) + J_{\uparrow}(B)}, \quad (10)$$

where  $J_{\uparrow}$  ( $J_{\downarrow}$ ) is the spin-up (spin-down) current density. On the other hand, in the absence of external magnetic field, the Zeeman splitting of the conduction electrons  $V_s$  and the spin dependent potential  $V_{\sigma_z}(z)$  are zero. In this case, the effective potential reduces to  $U_{\sigma_z}(z, 0) = V_x(z) - eV_a z/d$  which is spin-independent. Thus, by using  $U_{\sigma_z}(z, 0)$  and a procedure completely analogous to the one used for the case of  $B \neq 0$ , one can obtain the following formula for the total electric current density [17]

$$J(0) = 2 \left( \frac{em^* k_B T}{4\pi^2 \hbar^3} \right) \int_0^{+\infty} T_{\sigma_z}(E_z, 0, V_a) \ln \left\{ \frac{1 + \exp[(E_F - E_z)/k_B T]}{1 + \exp[(E_F - E_z - eV_a)/k_B T]} \right\} dE_z. \quad (11)$$

The factor two is due to the degeneracy of the electron spin in the case of  $B = 0$ . Although the transverse momentum  $\mathbf{k}_{\parallel}$  was not appeared in the above equation, the effects of the summation over  $\mathbf{k}_{\parallel}$  have been considered in our calculations. Here, we mention again that the effective mass is independent of layer. When taking both the transverse motion and the layer-dependent effective mass of the electron into account, the transmission coefficient can have a pronounced dispersion in  $\mathbf{k}_{\parallel}$  space [18]. In this case, one cannot simply reduce the 3D Schrödinger equation to the 1D equation and integrate the  $\mathbf{k}_{\parallel}$  to obtain the current density, as we did here.

The linear conductances per unit area are given by  $G(0) = J(0)/V_a$  and  $G(B) = \sum_{\sigma_z} J_{\sigma_z}(B)/V_a$  for  $B = 0$  and  $B \neq 0$ , respectively. Therefore, the tunnel magnetoresistance (TMR) or magnetoresistance ratio in such heterostructures can be described quantitatively by

$$\text{TMR} = \frac{G(0) - G(B)}{G(B)}$$

$$= \frac{J(0)}{J_{\uparrow}(B) + J_{\downarrow}(B)} - 1. \quad (12)$$

In next section, we will present the numerical results for  $J_{\sigma}$ ,  $P$  and TMR in terms of Mn concentration.

### III. RESULTS AND DISCUSSION

In our numerical calculation we have taken the following values:  $m^* = 0.16 m_e$  ( $m_e$  is the mass of the free electron),  $E_F = 5$  meV,  $B = 4$  T,  $g_s = 1.1$ ,  $T = 2.2$  K,  $T_0 = 1.7$  K, and  $N_0\alpha = -0.26$  eV [19]. Fig. 2(a)-(d) show the dependence of spin-up current densities on the Mn concentration for several choices of  $d$  and  $V_a$ . In all of the widths of the paramagnetic layer, for a fixed value of Mn concentration, the spin-up current density increases with the applied voltage. With increasing the Mn concentration ( $x > 0.043$ ), the spin-up electrons see a higher potential barrier, while with increasing the width of the paramagnetic layer, these electrons see a thicker potential barrier. Thus in both cases, the tunneling probability for this group of electrons decreases and this leads to a reduction of the current density. From the figures, we also find that, for  $d = 200$  nm and  $x > 0.055$ , the transmission for spin-up electrons is completely suppressed. On the other hand, with increasing the applied voltage, the potential barrier tilts and the effective width of the barrier becomes narrower; therefore, the spin-up current density increases, as shown in Fig. 2.

The dependence of spin-down current densities on the Mn concentration is shown in Fig. 3(a)-(d) for several values of  $d$  and  $V_a$ . For small widths of the paramagnetic layer, the variations of the current density are relatively small with an oscillatory behavior. These variations increase with the width  $d$ . Qualitatively, the voltage dependence of spin-down current density is similar to the spin-up one. This means that both spin current densities increase with the applied voltage. We should note that at  $x = 0$  the current densities are nearly spin-independent, because  $V_{\sigma_z}$  is zero and  $V_s$  is very small. With increasing  $d$  and  $x$ , peaks are observed in the spin-down current densities. The reason is that, the paramagnetic layer behaves as a quantum well for spin-down electrons; thus, the enhancement of the width of the paramagnetic layer, varies and shifts the position of the resonant states formed in the well to the lower energy region. This leads to the formation of peaks in the spin-down current densities [20].

In Fig. 4(a)-(d) we show the spin polarization for electrons traversing the heterostructure as a function of  $x$  for various values  $d$ . According to the above discussion, for  $x = 0$  the spin-up and spin-down current densities have equal values, hence the spin polarization is zero. As the Mn concentration increases, the spin-down current density first decreases, while the spin-up one is approximately constant; therefore, the spin polarization is negative. On further increasing the Mn concentration, the spin-up current density decreases exponentially; however the spin-down one can increase and when  $J_{\uparrow}$  vanishes,  $J_{\downarrow}$  has non-zero values. Consequently, the spin polarization becomes positive and increases for these values of the Mn concentration. It is also important to note that, for widths near 200 nm, the spin polarization approaches 100%, which shows that, the system acts as a spin filter.

The magnetoresistance ratio of  $\text{ZnSe}/\text{Zn}_{1-x}\text{Mn}_x\text{Se}/\text{ZnSe}$  heterostructures is another quantity which is sensitive to the Mn concentration. In Fig. 5(a)-(d) the TMR is plotted as a function of  $x$ . With increasing the width of  $\text{Zn}_{1-x}\text{Mn}_x\text{Se}$  layer, a peak appears in the TMR curves. This peak is shifted slowly towards lower values of the Mn concentration  $x$ , and its height increases with the width. From the figures, it is clear that the sign of TMR can be positive when  $G(0) > G(B)$  or negative when  $G(0) < G(B)$ . The reason of negative TMR can be understood by considering the effects of Mn concentration on spin transport in such heterostructures. With increasing the Mn content ( $x > 0.043$ ), the conduction band offset increases and the paramagnetic layer acts as a barrier for both spin-up and spin-down electrons in zero magnetic field. On applying a magnetic field, however, the spin-down electrons see a quantum well (when  $V_x + V_{\sigma_z} < 0$ ) and the current density for such electrons increases. Hence,  $G(0) < G(B)$  and TMR becomes negative. The results also show that, for a fixed width of the paramagnetic layer, the electron-spin polarization and the TMR curves do not depend strongly on the applied voltage, as shown in Figs. 4 and 5.

Guo *et al.* [11], studied the effects of zero-field conduction band offset on spin transport with  $V_x = -5, 0, +5$  meV and  $x = 0.05$ . They found that, for  $V_x = +5$  meV the spin currents are highly polarized, while, for  $V_x = -5$  meV the spin polarization is very low. Our present results based on the experimental data, however, indicate that the conduction band offset depends on the Mn concentration. Thus, in order to understand the correct description of the effects of the conduction band offset on spin transport, the dependence of this quantity on the Mn concentration was included. It is clear that the width of the paramagnetic layer is also one of the main factors in spin-polarization of the output current of the system.



Therefore, the obtained results clearly illustrate that the current densities and hence the degree of spin polarization and the TMR can be tuned by changing the Mn concentration and/or the width of the paramagnetic layer.

#### IV. SUMMARY

In this paper, using the transfer matrix method and the effective-mass approximation we investigated the ballistic spin-polarized transport in  $\text{ZnSe}/\text{Zn}_{1-x}\text{Mn}_x\text{Se}/\text{ZnSe}$  heterostructures. We examined the effects of Mn concentration, the width of the paramagnetic layer, and the external magnetic and electric fields on the spin current densities, the electron-spin polarization and the TMR. The numerical results show that the zero-field conduction band offset which varies with the Mn concentration, plays an important role in the spin current densities. The spin polarization and the TMR are not very sensitive to the applied voltage. However, by adjusting the Mn concentration and the width of the paramagnetic layer, the output current exhibits a nearly 100% spin polarization, and also the sign of the TMR can be positive or negative. The presented results may be helpful from a technological application point of view such as the generation of spin-polarized injection electrons.

- 
- [1] G.A. Prinz, Science 282 (1998) 1660.
  - [2] S.A. Wolf, D.D. Awschalom, R.A. Buhrman, J.M. Daughton, S von Molnár, M.L. Roukes, A.Y. Chtchelkanova, D.M. Treger, Science 294 (2001) 1488.
  - [3] G. Schmidt, L.W. Molenkamp, A.T. Filip, B.J. van Wees, Phys. Rev. B 62 (2000) R4790.
  - [4] J.K. Furdyna, J. Appl. Phys. 64 (1988) R29.
  - [5] Y. Ohno, D.K. Yong, B. Beschoten, F. Matsukura, H. Ohno, D.D. Awschalom, Nature 402 (1999) 790.
  - [6] R. Fiederling, G. Reuscher, W. Ossau, G. Schmidt, A. Waag, L.W. Molenkamp, Nature (London) 402 (2000) 787.
  - [7] G. Schmidt, G. Richter, P. Grabs, D. Ferrand, L.W. Molenkamp, Phys. Rev. Lett. 87 (2001) 22703.
  - [8] A. Slobodskyy, C. Gould, T. Slobodskyy, C.R. Becker, G. Schmidt, L.W. Molenkamp, Phys.

- Rev. Lett. 90 (2003) 246601.
- [9] M. Syed, G.L. Yang, J.K. Furdyna, M. Dobrowolska, S. Lee, L.R. Ram-Mohan, Phys. Rev. B 66 (2002) 075213.
  - [10] J.C. Egues, Phys. Rev. Lett. 80 (1998) 4578.
  - [11] Y. Guo, H. Wang, B.L. Gu, Y. Kawazoe, J. Appl. Phys. 88 (2000) 6614.
  - [12] K. Chang, F.M. Peeters, Solid State Commun. 120 (2001) 181.
  - [13] F. Zhai, Y. Guo, B.L. Gu, J. Appl. Phys. 90 (2001) 1328.
  - [14] N. Dai, L.R. Ram-Mohan, H. Luo, G.L. Yang, F.C. Zhang, M. Dobrowolska, J.K. Furdyna, Phys. Rev. B 50 (1994) 18153, and references therein.
  - [15] D.D. Awschalom, N. Samarth, J. Magn. Magn. Mater. 200 (1999) 130.
  - [16] S.S. Allen, S.L. Richardson, J. Appl. Phys. 79 (1996) 886.
  - [17] C.B. Duke, Tunneling Phenomena in Solids, ed. Burstein E and Lundquist S (Plenum, New York) (1969).
  - [18] A. Voskoboynikov, S.S Liu, and C.P. Lee, Phys. Rev. B 58 (1998) 15397.
  - [19] B. König, U. Zehnder, D.R. Yakovlev, W. Ossau, T. Gerhard, M. Keim, A. Waag, G. Landwehr, Phys. Rev. B 60 (1999) 2653.
  - [20] A. Saffarzadeh, M. Bahar, M. Banihasan, Physica E 27 (2005) 462.

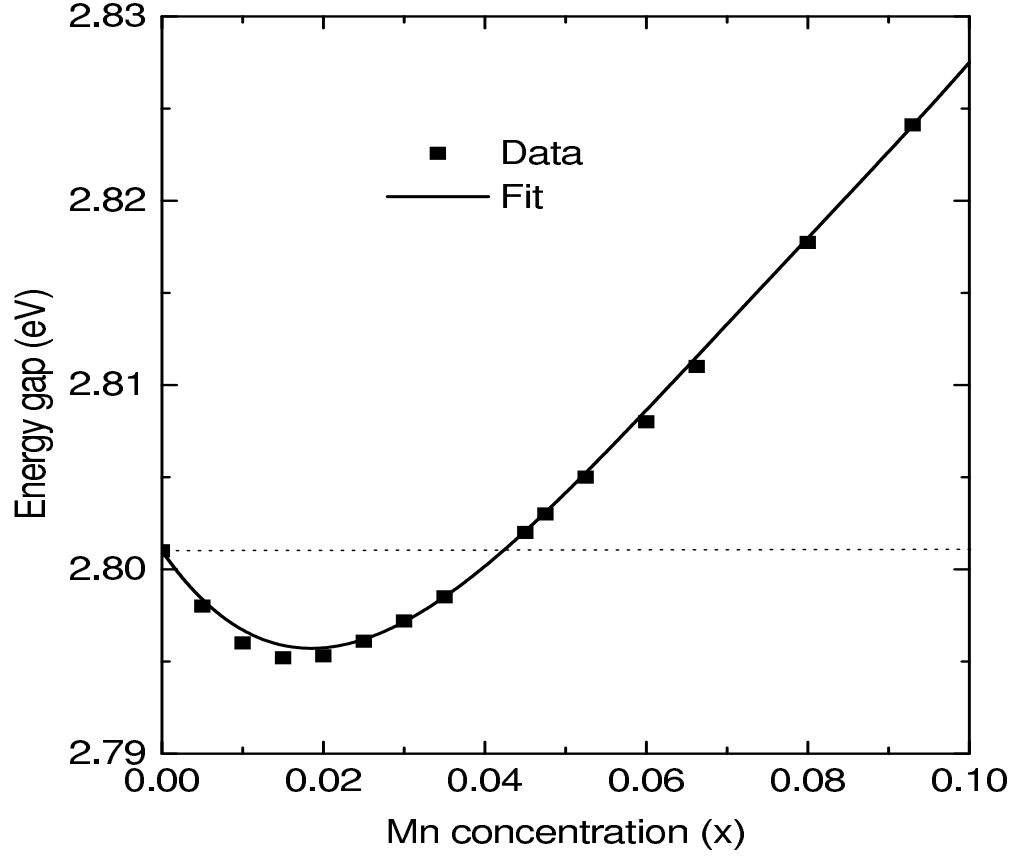


FIG. 1: Energy gap of  $\text{Zn}_{1-x}\text{Mn}_x\text{Se}$  as a function of Mn concentration  $x$  at  $T=2.2$  K. The experimental data (full squares) is taken from [14]. The solid curve is a fit to the data.

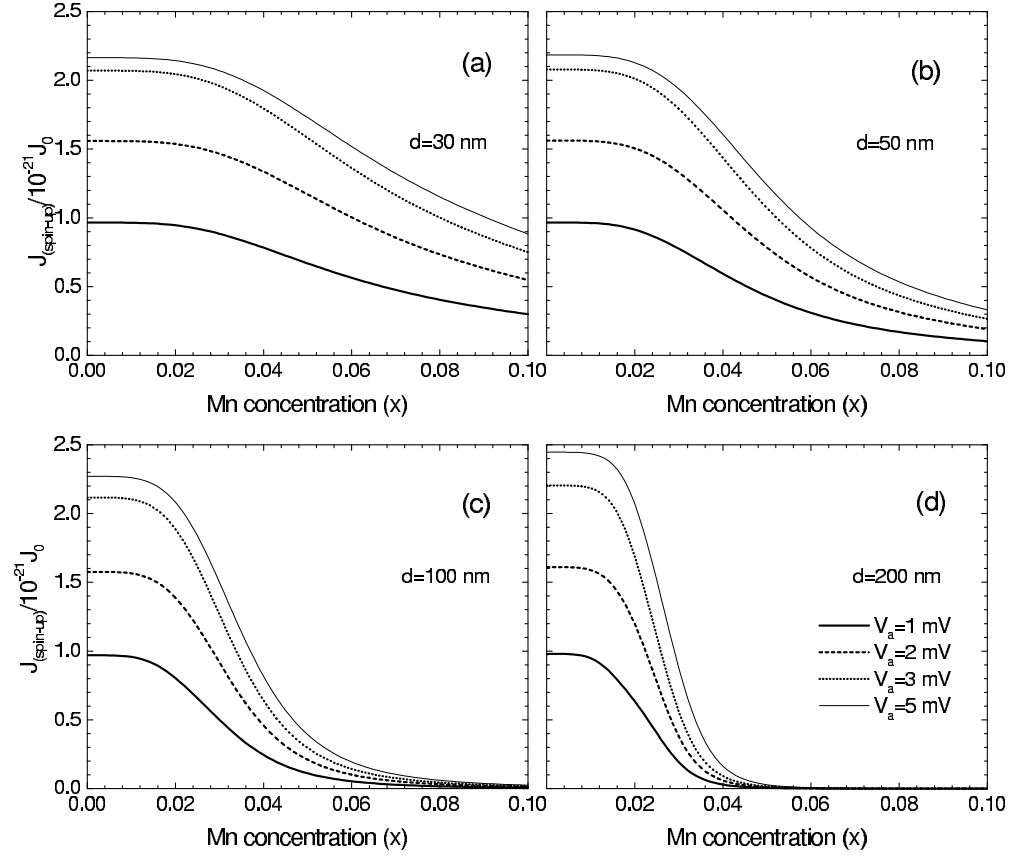


FIG. 2: Spin-up current densities as a function of Mn concentration  $x$  for different applied voltages and widths of  $\text{Zn}_{1-x}\text{Mn}_x\text{Se}$  layer.

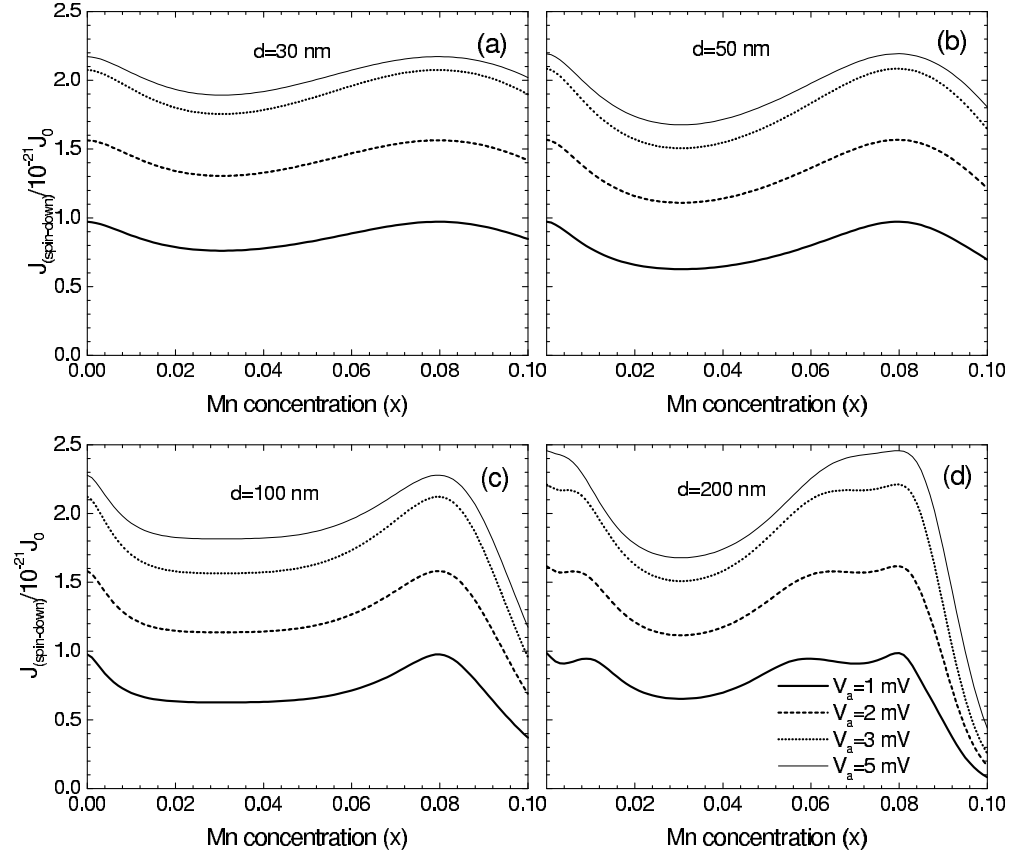


FIG. 3: Spin-down current densities as a function of Mn concentration  $x$  for different applied voltages and widths of  $\text{Zn}_{1-x}\text{Mn}_x\text{Se}$  layer.

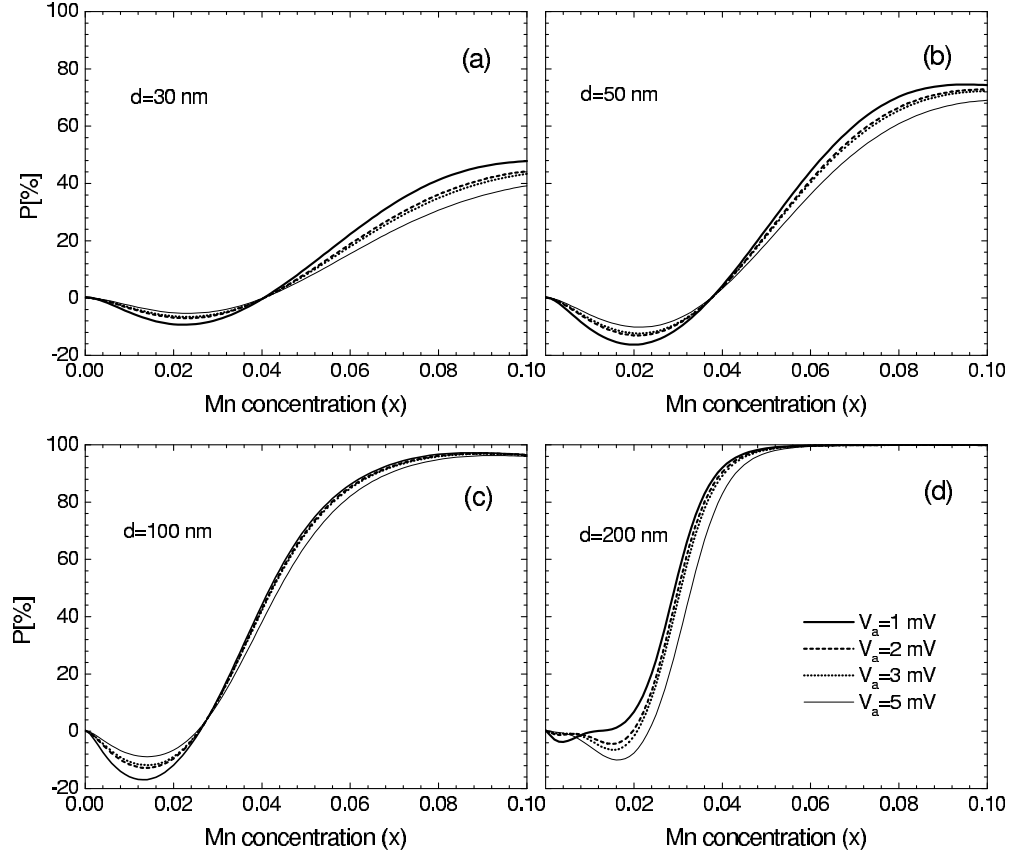


FIG. 4: Electron-spin polarization  $P$  as a function of Mn concentration  $x$  for different applied voltages and widths of  $\text{Zn}_{1-x}\text{Mn}_x\text{Se}$  layer.

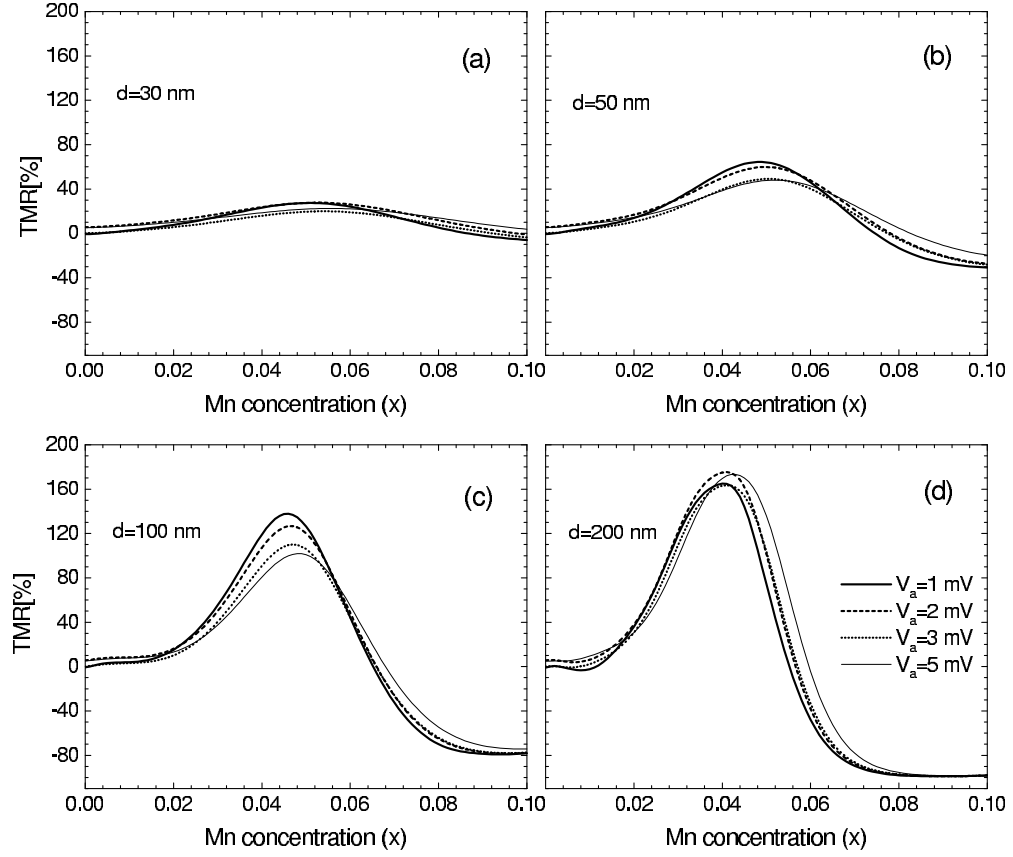


FIG. 5: TMR as a function of Mn concentration  $x$  for different applied voltages and widths of  $\text{Zn}_{1-x}\text{Mn}_x\text{Se}$  layer.